This article was downloaded by: [Institute Of Atmospheric Physics]
On: 09 December 2014, At: 15:32
Publisher: Taylor & Francis
Informa Ltd Registered in England and Wales Registered Number: 1072954 Registered office: Mortimer House, 37-41 Mortimer Street, London W1T 3JH, UK

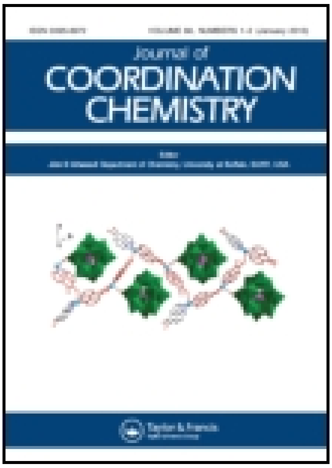

CrossMark
Click for updates

Journal of Coordination Chemistry
Publication details, including instructions for authors and subscription information:
http://www.tandfonline.com/loi/gcoo20

Four organic-inorganic compounds based on polyoxometalates: crystal structures and catalytic epoxidation of styrene

Chunling Wang[ab], Yuanhang Ren[a], Sujiao Feng[a], Zuping Kong[a], Yichen Hu[a], Bin Yue[a], Mingli Deng[a] & Heyong He[a]

[a] Shanghai Key Laboratory of Molecular Catalysis and Innovative Materials, Department of Chemistry, Collaborative Innovation Center of Chemistry for Energy Materials, Fudan University, Shanghai, PR China

[b] Low Carbon Energy Conversion Technology Center, Shanghai Advanced Research Institute, Chinese Academy of Sciences, Shanghai, PR China

Accepted author version posted online: 07 Feb 2014.Published online: 05 Mar 2014.

To cite this article: Chunling Wang, Yuanhang Ren, Sujiao Feng, Zuping Kong, Yichen Hu, Bin Yue, Mingli Deng & Heyong He (2014) Four organic-inorganic compounds based on polyoxometalates: crystal structures and catalytic epoxidation of styrene, Journal of Coordination Chemistry, 67:3, 506-521, DOI: 10.1080/00958972.2014.892592

To link to this article: http://dx.doi.org/10.1080/00958972.2014.892592

PLEASE SCROLL DOWN FOR ARTICLE

Taylor & Francis makes every effort to ensure the accuracy of all the information (the "Content") contained in the publications on our platform. However, Taylor & Francis, our agents, and our licensors make no representations or warranties whatsoever as to the accuracy, completeness, or suitability for any purpose of the Content. Any opinions and views expressed in this publication are the opinions and views of the authors, and are not the views of or endorsed by Taylor & Francis. The accuracy of the Content should not be relied upon and should be independently verified with primary sources of information. Taylor and Francis shall not be liable for any losses, actions, claims, proceedings, demands, costs, expenses, damages, and other liabilities whatsoever or howsoever caused arising directly or indirectly in connection with, in relation to or arising out of the use of the Content.

This article may be used for research, teaching, and private study purposes. Any substantial or systematic reproduction, redistribution, reselling, loan, sub-licensing, systematic supply, or distribution in any form to anyone is expressly forbidden. Terms & Conditions of access and use can be found at http://www.tandfonline.com/page/terms-and-conditions

Downloaded by [Institute Of Atmospheric Physics] at 15:32 09 December 2014

Journal of Coordination Chemistry, 2014
Vol. 67, No. 3, 506–521, http://dx.doi.org/10.1080/00958972.2014.892592

Taylor & Francis
Taylor & Francis Group

Downloaded by [Institute Of Atmospheric Physics] at 15:32 09 December 2014

Four organic–inorganic compounds based on polyoxometalates: crystal structures and catalytic epoxidation of styrene

CHUNLING WANG†‡, YUANHANG REN†, SUJIAO FENG†, ZUPING KONG†, YICHEN HU†, BIN YUE*†, MINGLI DENG† and HEYONG HE*†

†Shanghai Key Laboratory of Molecular Catalysis and Innovative Materials, Department of Chemistry, Collaborative Innovation Center of Chemistry for Energy Materials, Fudan University, Shanghai, PR China
‡Low Carbon Energy Conversion Technology Center, Shanghai Advanced Research Institute, Chinese Academy of Sciences, Shanghai, PR China

(*Received 10 November 2013; accepted 14 January 2014*)

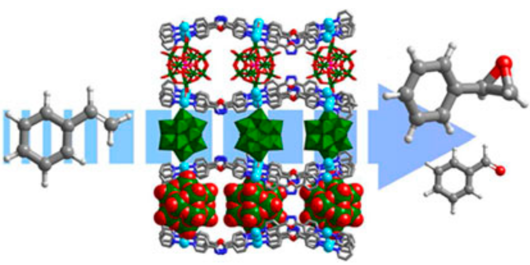

Four organic–inorganic hybrid compounds were hydrothermally synthesized based on polyoxometalates, copper salts, and 2,5-bis(4-pyridyl)-1,3,4-oxadiazole or isonicotinic acid ligands. Among those four compounds, compound **2**, $[Cu(4\text{-bpo})]_4[P_2W_{18}O_{62}][N(CH_3)_4]_2\cdot 6H_2O$, showed the best catalytic activity for heterogeneous epoxidation of styrene to styrene oxide using *tert*-butyl hydroperoxide as oxidant.

Four compounds based on polyoxometalates, $[Cu(4\text{-bpo})(H_2O)][Cu_2(\mu_2\text{-Cl})(4\text{-bpo})_2(H_2O)][SiW_{12}O_{40}][N(CH_3)_4]_2\cdot H_2O$ (**1**), $[Cu(4\text{-bpo})]_4[P_2W_{18}O_{62}][N(CH_3)_4]_2\cdot 6H_2O$ (**2**), $[Cu_2(\mu_2\text{-OH})(4\text{-bpo})_2(Hina)(H_2O)_2]_2[P_2W_{18}O_{62}]\cdot 4H_2O$ (**3**), and $[Cu_2(Hina)_4(H_2O)_2][H_2P_2W_{18}O_{62}](Hina)\cdot 11H_2O$ (**4**) (4-bpo=2,5-bis(4-pyridyl)-1,3,4-oxadiazole, ina=isonicotinic acid), have been hydrothermally synthesized and characterized by elemental analysis, IR, and single-crystal X-ray diffraction. The 3-D framework of **1** is composed by Keggin-type polyoxoanions $\{SiW_{12}\}$ and two types of infinite chains, $\{Cu(4\text{-bpo})(H_2O)\}_n$ and $\{Cu_2(\mu_2\text{-Cl})(4\text{-bpo})_2(H_2O)\}_n$, through hydrogen bonds. Compound **2** has a 3-D rigid framework which is fabricated by Wells–Dawson type polyoxoanions $\{P_2W_{18}\}$ and Cu-(4-bpo) chains through covalent bonds. Compound **3** contains an infinite $\{Cu_2(\mu_2\text{-OH})(4\text{-bpo})_2(Hina)(H_2O)_2\}_n$ double-chain and $\{P_2W_{18}\}$ polyoxoanions immobilized in the voids between the chains. Compound **4** exhibits a 3-D supramolecular network directed by hydrogen bonds between $\{P_2W_{18}\}$ polyoxoanions and the double paddle-wheel $\{Cu_2(Hina)_4(H_2O)_2\}$. Compounds

*Corresponding authors. Email: yuebin@fudan.edu.cn (B. Yue); heyonghe@fudan.edu.cn (H. He)

© 2014 Taylor & Francis

1–4 were tested as heterogeneous catalysts for the epoxidation of styrene using *tert*-butyl hydroperoxide (TBHP) as oxidant. The compounds show catalytic activity with **2** giving the highest yield of styrene oxide.

Keywords: Polyoxometalates; Organic–inorganic hybrid; Crystal structure; Heterogeneous catalyst; Styrene epoxidation

Downloaded by [Institute Of Atmospheric Physics] at 15:32 09 December 2014

1. Introduction

Polyoxometalates (POMs) have attracted attention as catalysts due to their application as acid and redox bifunctional properties under mild conditions [1]. POMs-based catalysts have been applied to several large-scale industrial processes [2]. However, most POMs-based catalysts are homogeneous, although their heterogeneous catalysts would be preferable for separation and reusability [3].

One approach to obtain heterogeneous catalysts is to immobilize the homogeneous catalyst on an insoluble support [4]. Water-soluble POMs have been supported on different types of substrates, such as resin [5], active carbon [6], neutral or acidic oxides [7], mesoporous materials [8], and coordination polymers [9]. However, these supported POMs catalysts still have some limitations: (1) the supports must be acidic or neutral to avoid decomposition of POMs [10]; (2) the weak interactions (electrostatic force or molecular interaction) between supports and POMs may induce leaching of the active species into polar media; (3) the inevitable aggregation of POMs on the supports during preparation and reaction may reduce catalytic activity; and (4) unclear structure of the active sites results in difficulty for mechanistic study. Therefore, developing new heterogeneous POMs-based catalysts still is a challenge.

Self-assembly of organic–inorganic hybrid compounds based on POMs has been an attractive research area [11]. The dynamic structures of these compounds can be adjusted over a wide range by using different kinds of POMs, metal ions, and organic ligands. Structures with diversified porous, acidic, and redox properties can be designed by tuning the precursors and controlling the synthesis conditions [12]. The POMs are immobilized uniformly in their frameworks as inorganic building blocks through hydrogen or covalent bonds which lead to high thermal stability and water resistance [13]. Also, transition metals in the organic–inorganic hybrid structure as co-catalytic active or assisting species could improve their catalytic activity. The structural details of organic–inorganic hybrid POMs, such as the type of POMs, the coordination environment of metal ions, the linking mode of organic ligands, and the porosity are clarified by single-crystal X-ray diffraction (XRD). All these features make hybrid POMs compounds good candidates as a new type of heterogeneous POMs-based catalysts. Although a large number of organic–inorganic hybrid POMs have been reported, investigation of these materials in heterogeneous catalytic processes is still in its infancy [14].

Recently, several heterogeneous catalytic reactions have been reported based on POMs. Long *et al.* reported the oxidation of ethylbenzene, 1-phenylethanol, and styrene with a series of organic–inorganic hybrid catalysts based on Keggin-type polyoxoanions and 4,4′-bipyridine [15]. Ali *et al.* reported the epoxidation of olefin over organic–inorganic hybrid compounds based on Anderson polyoxoanions [16] and Jia *et al.* investigated the catalytic activity for epoxidation of cyclooctene with *N*-heterocyclic-ligand-modified *β*-octamolybdates [17]. In previous work, we reported the synthesis of organic–inorganic hybrid compounds based on Keggin type $[SiW_{12}O_{40}]^{4-}$ and 3- or 4-bpo (3-bpo=2,5-bis(3-pyridyl)-1,3,4-oxadiazole, 4-bpo=2,5-bis(4-pyridyl)-1,3,4-oxadiazole) coordinated metal ions and investigation on their catalytic activity in epoxidation of styrene [18]. All of these catalysts displayed heterogeneous characteristics during the reaction. Herein, we report four new compounds based on Keggin and/or Wells–Dawson type POMs and copper coordination complexes with 4-bpo and/or isonicotinic acid (ina), formulated as $[Cu(4\text{-bpo})(H_2O)][Cu_2(\mu_2\text{-Cl})(4\text{-bpo})_2(H_2O)][SiW_{12}O_{40}][N(CH_3)_4]_2{\cdot}H_2O$ (**1**), $[Cu(4\text{-bpo})]_4[P_2W_{18}O_{62}][N(CH_3)_4]_2{\cdot}6H_2O$ (**2**), $[Cu_2(\mu_2\text{-OH})(4\text{-bpo})_2(Hina)(H_2O)_2]_2[P_2W_{18}O_{62}]{\cdot}4H_2O$ (**3**), and $[Cu_2(Hina)_4(H_2O)_2][H_2P_2W_{18}O_{62}](Hina){\cdot}11H_2O$ (**4**). Their catalytic activity for epoxidation of styrene was investigated which may provide useful information on the design of POM-based heterogeneous catalysts.

2. Experimental

2.1. *Materials and measurements*

$H_4SiW_{12}O_{40}{\cdot}19H_2O$ and $H_6P_2W_{18}O_{62}{\cdot}14H_2O$ were prepared according to the literature method and confirmed by IR spectroscopy [19]. Ligand 4-bpo was prepared according to literature procedures and confirmed by ^1H NMR spectroscopy [20]. Other reagents were purchased from commercial sources and used directly without purification. Elemental analyses were performed on an inductively coupled plasma IRIS Intrepid atomic-emission spectrometer (Si, P, W, and Cu) and Elementary Vario EL III microanalyser (C, H, and N). TG analysis was performed on a Perkin-Elmer TGA7 analyzer in air with a heating rate of 10 °C min^{-1} to determine the number of water molecules in **1–4**. IR spectra were recorded from 4000 to 400 cm^{-1} on a Nicolet Nexus 470 FTIR spectrometer using KBr pellets. X-ray powder diffraction patterns were obtained using a Bruker D4 diffractometer at 40 kV and 40 mA with Cu-K*α* radiation ($\lambda = 1.5418$ Å). XPS experiments were carried out on a Perkin-Elmer PHI-5000C ESCA system with Mg-K*α* radiation ($h\nu = 1253.6$ eV).

2.2. *Preparation of $[Cu(4\text{-bpo})(H_2O)][Cu_2(\mu_2\text{-Cl})(4\text{-bpo})_2(H_2O)][SiW_{12}O_{40}][N(CH_3)_4]_2{\cdot}H_2O$*

A mixture of $H_4SiW_{12}O_{40}{\cdot}19H_2O$ (0.32 g, 0.10 mM), $CuCl_2{\cdot}2H_2O$ (0.034 g, 0.20 mM), 4-bpo (0.045 g, 0.20 mM), and H_2O (10 mL), adjusted with 25% $(CH_3)_4NOH$ solution to pH 8.0, was sealed in a 15 mL Teflon-lined reactor. The mixture was heated to 160 °C for three days and then cooled to room temperature at 10 °C h^{-1}. Orange crystals were obtained in 49% yield on the basis of W. $C_{44}H_{54}N_{14}SiClCu_3W_{12}O_{46}$ (3975.22): Calcd C 13.29, H 1.37, N 4.93, Si 0.71, W 55.50, Cu 4.80, Cl 0.89; found C 13.12, H 1.50, N 4.69, Si 0.75, W 55.37, Cu 4.88.

2.3. *Preparation of $[Cu(4\text{-bpo})]_4[P_2W_{18}O_{62}][N(CH_3)_4]_2{\cdot}6H_2O$*

A mixture of $K_6P_2W_{18}O_{62}{\cdot}14H_2O$ (0.24 g, 0.050 mM), $Cu(NO_3)_2{\cdot}3H_2O$ (0.048 g, 0.20 mM), 4-bpo (0.045 g, 0.20 mM), and H_2O (10 mL), adjusted with 25% $(CH_3)_4NOH$ solution to pH 8.0, was sealed in a 15 mL Teflon-lined reactor. The mixture was heated to

Downloaded by [Institute Of Atmospheric Physics] at 15:32 09 December 2014

160 °C for three days and then cooled to room temperature at 10 °C h^{-1}. Orange crystals were obtained in 69% yield on the basis of W. $C_{56}H_{68}N_{18}P_2Cu_4W_{18}O_{72}$ (5770.47): Calcd C 11.66, H 1.19, N 4.37, P 1.07, W 57.35, Cu 4.40; found C 11.48, H 1.28, N 4.21, P 1.12, W 57.28, Cu 4.33.

2.4. *Preparation of [$Cu_2(\mu_2$-OH)(4-bpo)$_2$(Hina)($H_2O)_2]_2[P_2W_{18}O_{62}]\cdot 4H_2O$*

A mixture of $K_6P_2W_{18}O_{62}\cdot 14H_2O$ (0.24 g, 0.050 mM), $Cu(NO_3)_2\cdot 3H_2O$ (0.048 g, 0.20 mM), 4-bpo (0.045 g, 0.20 mM), ina (0.025 g, 0.20 mM), and H_2O (10 mL), adjusted with 25% $(CH_3)_4NOH$ solution to pH 6.0, was sealed in a 15 mL Teflon-lined reactor. The mixture was heated to 160 °C for three days and then cooled to room temperature at 10 °C h^{-1}. Blue crystals were obtained in 47% yield on the basis of W. $C_{60}H_{60}N_{18}P_2Cu_4W_{18}O_{80}$ (5938.44): Calcd C 12.14, H 1.02, N 4.24, P 1.04, W 55.72, Cu 4.28; found C 11.89, H 1.21, N 4.07, P 0.93, W 55.61, Cu 4.19.

2.5. *Preparation of [$Cu_2(Hina)_4(H_2O)_2][H_2P_2W_{18}O_{62}]$(Hina)·11$H_2O$*

A mixture of $K_6P_2W_{18}O_{62}\cdot 14H_2O$ (0.48 g, 0.10 mM), $Cu(NO_3)_2\cdot 3H_2O$ (0.048 g, 0.20 mM), ina (0.062 g, 0.50 mM), and H_2O (10 mL), adjusted with 25% $N(CH_3)_4OH$ solution to pH 4.0, was sealed in a 15 mL Teflon-lined reactor. The mixture was heated to 160 °C for three days and then cooled to room temperature at 10 °C h^{-1}. Blue crystals were obtained in 41% yield on the basis of W. $C_{30}H_{53}N_5P_2Cu_2W_{18}O_{85}$ (5341.88): Calcd C 6.74, H 1.00, N 1.31, P 1.16, W 61.95, Cu 2.38; found C 6.58, H 1.23, N 1.12, P 1.21, W 61.83, Cu 2.29.

2.6. *Catalysis*

Epoxidation of styrene (0.10 mL, 0.86 mM) was carried out in a 20 mL flask with a water-cooled condenser using aqueous 70 wt.% *tert*-butyl hydroperoxide (TBHP, 0.20 mL, 1.4 mM) as oxidant in acetonitrile (4 mL); 0.005 mM catalyst was added into the mixture at 343 K with stirring. The liquid organic products were quantified at certain intervals using gas chromatography (GC 9560) equipped with a flame ionization detector and a HP-5 capillary column (0.32 mm, 30 m, 0.25 μm) at 110 °C with He as the carrier gas after removal of the catalyst by centrifugation.

2.7. *Crystallographic data collection and determination*

The reflection intensities of **1–4** were collected on a Bruker SMART CCD diffractometer equipped with Mo-Kα graphite-monochromated radiation (λ = 0.71073 Å) at 293 K. Data reduction and cell refinement were performed with SAINT and the absorption correction program SADABS was employed to correct the data for absorption. The structures were solved by the direct method and refined using full-matrix least-squares treatment (SHELXTL-97) [21] with atomic coordinates and anisotropic thermal parameters for all non-hydrogen atoms. Hydrogens on 4-bpo and ina rings were introduced at calculated positions and included in the refinement riding on their respective parent. The crystal data and structure refinement results of **1–4** are summarized tables 1 and S1–S12.

Downloaded by [Institute Of Atmospheric Physics] at 15:32 09 December 2014

Downloaded by [Institute Of Atmospheric Physics] at 15:32 09 December 2014

Table 1. Crystal and refinement data for **1–4**.

Compounds	**1**	**2**	**3**	**4**
Empirical formula	$C_{44}H_{54}N_{14}SiClCu_3W_{12}O_{46}$	$C_{56}H_{68}N_{18}P_2Cu_4W_{18}O_{72}$	$C_{60}H_{60}N_{18}P_2Cu_4W_{18}O_{80}$	$C_{30}H_{53}N_5P_2Cu_2W_{18}O_{85}$
Formula mass	3975.22	5770.47	5938.44	5341.88
T (K)	293(2)	293(2)	293(2)	293(2)
Wavelength (Å)	0.71073	0.71073	0.71073	0.71073
Crystal system	Triclinic	Monoclinic	Orthorhombic	Orthorhombic
Space group	*P–1*	*C2/m*	*Cmc2₁*	*Pnma*
a (Å)	13.616(4)	28.200(9)	15.164(5)	29.739(10)
b (Å)	14.252(4)	26.802(9)	26.274(9)	19.127(7)
c (Å)	22.046(6)	14.625(5)	27.603(9)	18.268(6)
α (°)	75.313(4)	90.00	90.00	90.00
β (°)	80.192(4)	101.475(5)	90.00	90.00
γ (°)	68.120(4)	90.00	90.00	90.00
V (Å^3)	3826(2)	10,833(6)	10,997(6)	10,391(6)
Z	2	4	4	4
No. of reflections for refinement	10,866	27,828	29,590	42,648
GOF on F^2	0.897	0.922	0.977	0.968
R_1 ($I > 2\sigma(I)$)[a]	0.0535	0.0449	0.0513	0.0517
wR_2 (all data)[b]	0.1269	0.1094	0.1242	0.1433

[a] $R_1 = \sum||F_o| - |F_c||/\sum|F_o|$.
[b] $wR_2 = [\sum w(F_o^2 - F_c^2)^2/\sum w(F_o^2)^2]^{1/2}$.

Downloaded by [Institute Of Atmospheric Physics] at 15:32 09 December 2014

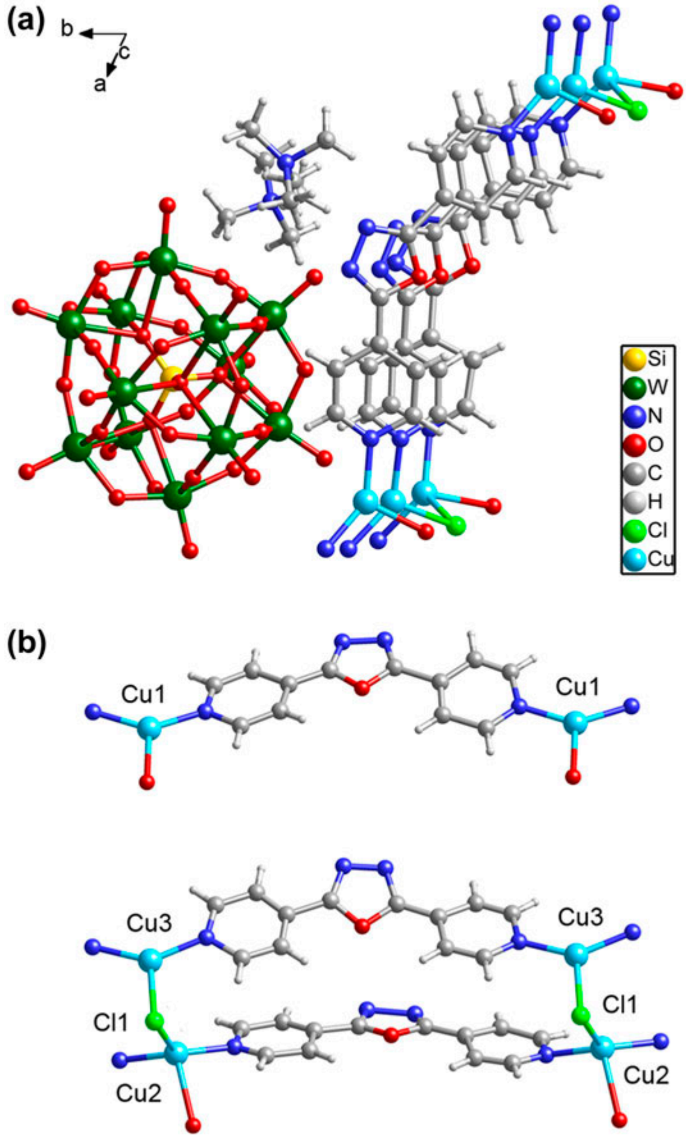

Figure 1. (a) Ball-stick representation of the packing mode of **1**. (b) Coordination environments of Cu1 and Cu3 in **1** (color code: Si, orange; W, dark green; N, blue; O, red; C, gray; H, white; Cl, light green; Cu, cyan (see http://dx.doi.org/10.1080/00958972.2014.892592 for color version)).

3. Results and discussion

3.1. *Crystal structure*

3.1.1. [Cu(4-bpo)(H$_2$O)][Cu$_2$(μ$_2$-Cl)(4-bpo)$_2$(H$_2$O)][SiW$_{12}$O$_{40}$][N(CH$_3$)$_4$]$_2$·H$_2$O (1). Single-crystal XRD analysis indicates that **1** consists of Keggin-type $[SiW_{12}O_{40}]^{4-}$ polyoxoanions, $\{Cu(4\text{-bpo})(H_2O)\}_n$ chains, $\{Cu_2(\mu_2\text{-Cl})(4\text{-bpo})_2(H_2O)\}_n$ chains, and $[N(CH_3)_4]^+$

Downloaded by [Institute Of Atmospheric Physics] at 15:32 09 December 2014

cations [figures 1(a) and S1, see online supplemental material at http://dx.doi.org/10.1080/00958972.2014.892592]. $[SiW_{12}O_{40}]^{4-}$ belongs to the classical Keggin-type structure with a central SiO_4 tetrahedron surrounded by four vertex-sharing W_3O_{13} trimers. The relevant W–O bond distances in the polyoxoanion can be classified into three groups of W–O_a, W–O_b and W–O_t with distances of 2.32(1)–2.43(1), 1.85(1)–1.96(1), and 1.70 (1)–1.73(1) Å, respectively. The difference of the distances in each group further implies the electrostatic force or hydrogen bond interactions between the polyoxoanions and the neighboring metal-organic chains.

There are three crystallographically independent copper centers. Cu1 is coordinated by two nitrogens of two 4-bpo and one water in a $\{CuN_2O\}$ triangle [figure 1(b)]. Cu2 is coordinated by two nitrogens of two 4-bpo ligands, one Cl, and one protonated oxygen to display a distorted $\{CuN_2ClO\}$ tetrahedral geometry. Cu3 is coordinated by two nitrogens of two 4-bpo ligands and one Cl in a $\{CuN_2Cl\}$ triangle [figure 1(b)]. Cu–O bond distances are 2.17(1)–2.59 Å. The bond angles of N–Cu–N are 135.3(9)°–139.7(7)° and N–Cu–O angles are 90.9°–112.1(6)°. Cl1 bridges Cu2 and Cu3 to form a binuclear copper cluster with an average Cu–Cl distance of 2.34 Å and the bond angles of Cl–Cu–N are 101.0(5)°–118.3(7)°. Bond valence sum [22, 12] calculation shows that the Cu centers are +1.

The 4-bpo molecules connect Cu ions side-by-side to form two types of infinite hybrid chains, $\{Cu(4\text{-bpo})(H_2O)\}_n$ (chain *A*) and $\{Cu_2(\mu_2\text{-Cl})(4\text{-bpo})_2(H_2O)\}_n$ (chain *B*), as shown in figure 2. Chains *A* and *B* are arranged in *AABBAABB* mode to form 2-D hybrid layers along the *ac* plane through *π*–*π* interactions. Adjacent *AA* or *BB* chains are related by an inversion center. $[SiW_{12}O_{40}]^{4-}$ and $[N(CH_3)_4]^+$ locate between the adjacent 2-D hybrid layers to form the 3-D framework structures through hydrogen bonds (figure 3).

3.1.2. $[Cu(4\text{-bpo})]_4[P_2W_{18}O_{62}][N(CH_3)_4]_2\cdot 6H_2O$ (2).

Single-crystal XRD analysis reveals that **2** exhibits a 3-D structure connected by $[P_2W_{18}O_{62}]^{6-}$ polyoxoanions and $\{Cu(4\text{-bpo})\}_n$ infinite chains as shown in figures 4 and S2. The classical Wells–Dawson type $\{P_2W_{18}\}$ polyoxoanion with virtual D_{3h} symmetry can be viewed as fusion of two A-type α-$\{PW_9\}$

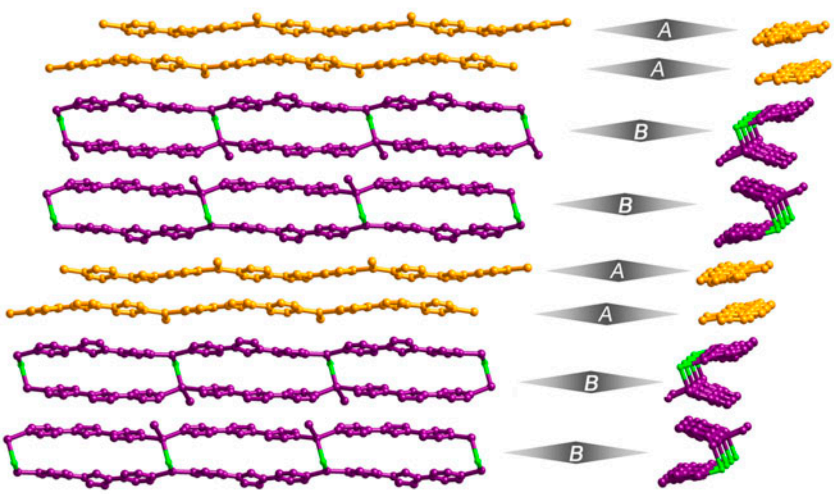

Figure 2. The packing mode of $\{Cu(4\text{-bpo})(H_2O)\}_n$ (chain *A*) and $\{Cu_2(\mu_2\text{-Cl})(4\text{-bpo})_2(H_2O)\}_n$ (chain *B*) in **1** viewed along the *b* (left) and *a* (right) axes.

Downloaded by [Institute Of Atmospheric Physics] at 15:32 09 December 2014

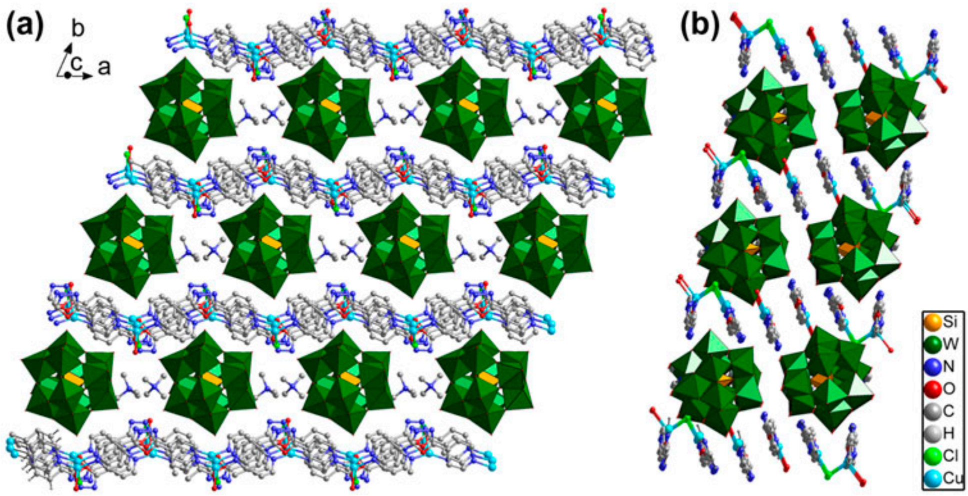

Figure 3. (a) Perspective view of 3-D structure of **1**. (b) The 3-D structure of **1** viewed along the *a* axis (color code: Si, orange; W, dark green; N, blue; O, red; C, gray; H, white; Cl, light green; Cu, cyan (see http://dx.doi.org/10.1080/00958972.2014.892592 for color version)).

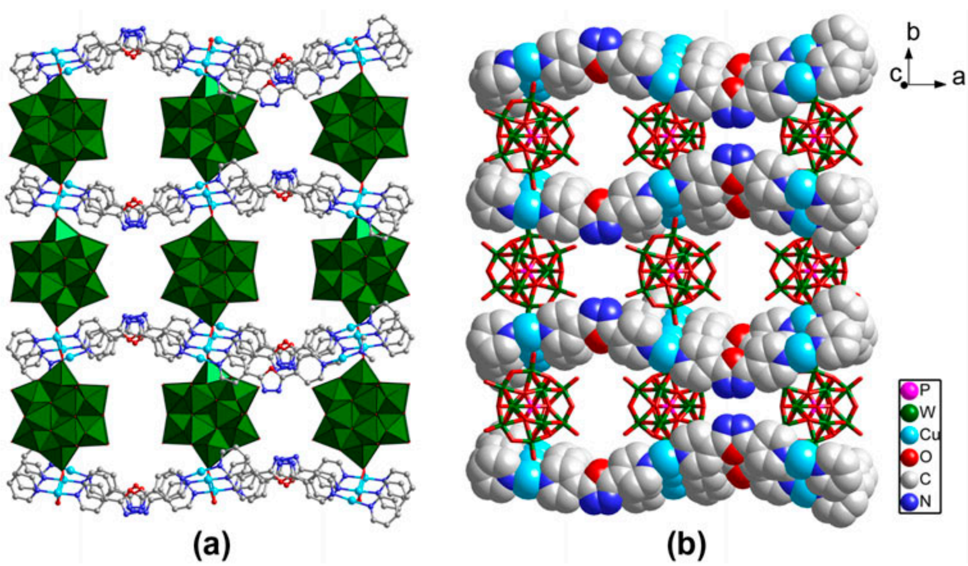

Figure 4. (a) Ball-stick and (b) space-filling representations of the 3-D structure of **2** (color code: P, purple; W, dark green; Cu, cyan; O, red; C, gray; N, blue (see http://dx.doi.org/10.1080/00958972.2014.892592 for color version)).

units, in which there are two types of tungstens including six as "polar" and twelve as "equatorial." Each $\{P_2W_{18}\}$ polyoxoanion coordinates to four coppers with two equatorial terminal oxygens, which results in severe distortion among the equatorial WO_6 octahedra with W–O_t(–Cu) distance elongated to 1.73(1) Å compared with 1.69(1)–1.72(1) Å of W–O_t in other equatorial sites. The coordination further leads to change of P–O distance in

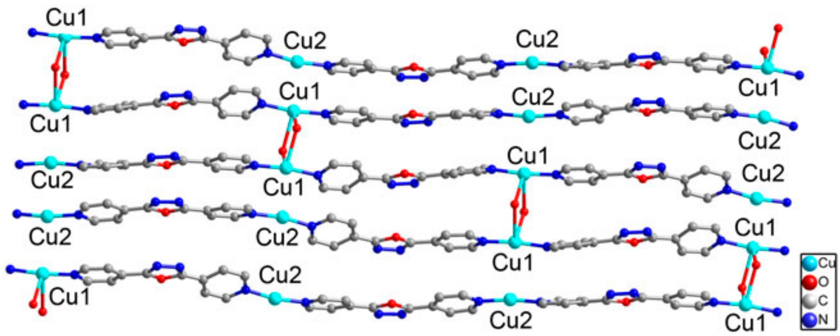

Figure 5. Ball-stick representation of the 2-D hybrid layer connected by Cu ions and 4-bpo in **2** (color code: Cu, cyan; O, red; C, gray; N, blue (see http://dx.doi.org/10.1080/00958972.2014.892592 for color version)).

PO_4 tetrahedra from 1.52(1) to 1.59(1) Å, however, the average P–O distance of 1.54 Å lies within the normal range.

There are two crystallographically independent Cu ions in **2**. Cu1 is four coordinate by two terminal oxygens from two $\{P_2W_{18}\}$ polyoxoanions and two N from two 4-bpo to form a seesaw coordination geometry. Cu2 is coordinated by two N of two 4-bpo linearly. The bond lengths are 1.88(1)–1.93(1) Å for Cu–N and 2.44(1)–2.70 Å for Cu–O. The N–Cu–N bond angles are 170.1(7)°–171.8(6)°. Bond valence sum [22] calculation indicates +1 Cu. The 4-bpo molecules are connected by coppers as bidentate ligands to form infinite chains, –Cu1-(4-bpo)-Cu2-(4-bpo)-Cu2-(4-bpo)-Cu1– (figure 5). Adjacent two 4-bpo molecules in the chain arrange alternately in an inversion-fashion. The chains are parallel to each other and further connect into 2-D wavy layers by terminal oxygens of $\{P_2W_{18}\}$ as μ_2-bridges through Cu1–O_t bonds. The distance between two Cu1 ions in adjacent chains is 4.05 Å.

Wells–Dawson type $\{P_2W_{18}\}$ polyoxoanions are connected into 1-D inorganic chains by binuclear Cu units through Cu1–O_t bonds as shown in figure 6. The inorganic chains extend along the *b* axis which is vertical to the Cu-(4-bpo) chains. Each polyoxoanion is connected to two Cu-(4-bpo) chains through two O_t–Cu1–N bridges which constructs the 3-D rigid framework of **2**. Only a few 3-D frameworks based on Wells–Dawson type polyoxoanions have been reported [23].

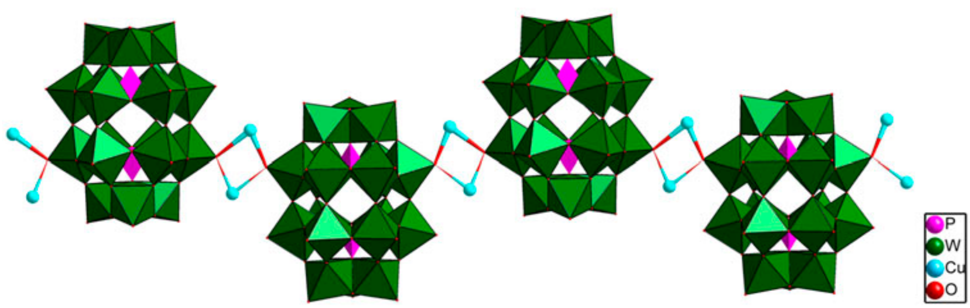

Figure 6. The Cu/Wells–Dawson inorganic chains linked by binuclear Cu units along the *b* axis in **2** (color code: P, purple; W, dark green; Cu, cyan; O, red (see http://dx.doi.org/10.1080/00958972.2014.892592 for color version)).

Downloaded by [Institute Of Atmospheric Physics] at 15:32 09 December 2014

Downloaded by [Institute Of Atmospheric Physics] at 15:32 09 December 2014

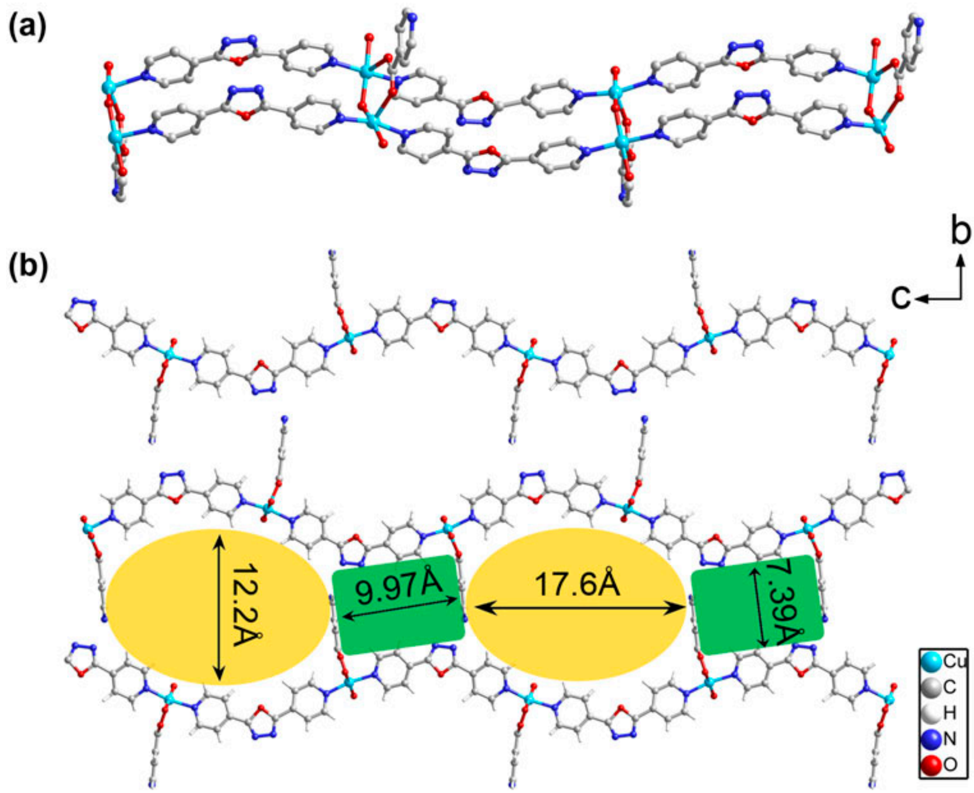

Figure 7. (a) The coordination environment of Cu in $\{Cu_2(\mu_2\text{-}OH)(4\text{-bpo})_2(Hina)(H_2O)_2\}_n$ double-chains and (b) ball-stick representations of 2-D supramolecular layer in **3** (color code: Cu, cyan; C, gray; H, white; N, blue; O, red (see http://dx.doi.org/10.1080/00958972.2014.892592 for color version)).

3.1.3. $[Cu_2(\mu_2\text{-}OH)(4\text{-bpo})_2(Hina)(H_2O)_2]_2[P_2W_{18}O_{62}]\cdot 4H_2O$ (3). Compound **3** contains $[P_2W_{18}O_{62}]^{6-}$ and infinite $\{Cu_2(\mu_2\text{-}OH)(4\text{-bpo})_2(Hina)(H_2O)_2\}_n$ double-chains (figures 7 and S3). The structure of **3** is similar to the one reported by Wang *et al.* [24] with minor difference in composition. In our synthesis, the reaction was carried out under a lower temperature with a higher yield for **3**.

There are two crystallographically independent Cu ions in **3**. Both are in similar square pyramidal geometry coordinated by two nitrogens of two 4-bpo molecules, one oxygen of ina, one bridging O towards another Cu, and one water. The bond lengths are 1.99(2)–2.10 (2) Å for Cu–N and 1.91(1)–2.22(1) Å for Cu–O. Bond valence sum [22] calculation shows that the Cu centers are +2 and O bridging the two Cu atoms is monoprotonated. The Cu and 4-bpo connect alternately to form an infinite 1-D chain. Two parallel chains are further bridged by ina and μ_2-OH to form a wavy hybrid double-chain $\{Cu_2(\mu_2\text{-}OH)(4\text{-bpo})_2(Hina)(H_2O)_2\}_n$ as shown in [figure 7(a)].

Two types of voids are formed between adjacent hybrid $\{Cu_2(\mu_2\text{-}OH)(4\text{-bpo})_2(Hina)(H_2O)_2\}_n$ chains as shown in [figure 7(b)]. The sizes of the opening are about 12.2 × 17.6 Å for the large void and 7.39 × 9.97 Å for the small one. The $\{P_2W_{18}\}$ polyoxoanions are immobilized uniformly in the large voids through C–H···O hydrogen bonds between C–H

Downloaded by [Institute Of Atmospheric Physics] at 15:32 09 December 2014

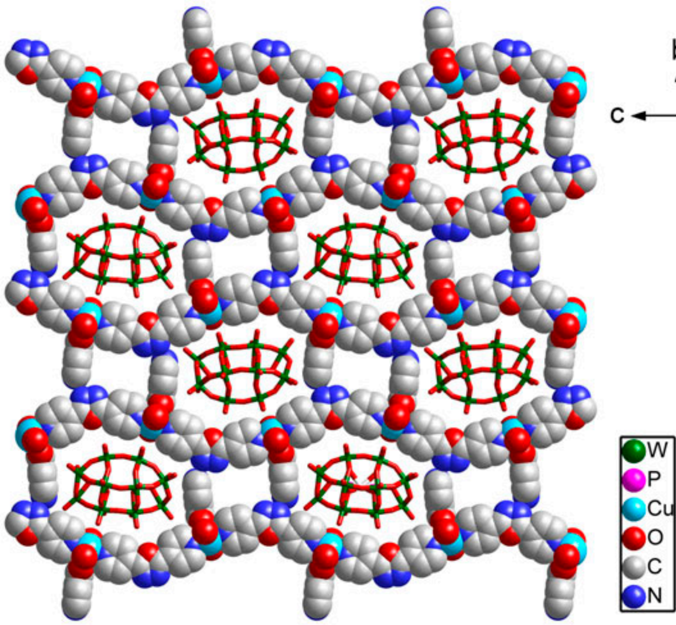

Figure 8. The arrangement of Wells–Dawson polyoxoanions between the 2-D supramolecular layers of **3** viewed along the *a* axis (color code: W, dark green; P, purple; Cu, cyan; O, red; C, gray; N, blue (see http://dx.doi.org/10.1080/00958972.2014.892592 for color version)).

of 4-bpo and oxygen of $\{P_2W_{18}\}$ (figures 8 and S4). The 3-D network of **3** is constructed through hydrogen bonding and π–π interactions.

3.1.4. Crystal structure of $[Cu_2(Hina)_4(H_2O)_2][H_2P_2W_{18}O_{62}](Hina)\cdot 11H_2O$ (4). Compound **4** is a 3-D supramolecule constructed by $[H_2P_2W_{18}O_{62}]^{4-}$ and $\{Cu_2(Hina)_4(H_2O)_2\}$ through hydrogen bonds. There are two crystallographically independent Cu ions in **4**. Each Cu is five coordinate in a square pyramidal geometry by four oxygens from four ina molecules and one water at the axial position. The Cu–O bond lengths are 1.96(1)–1.99(2) Å.

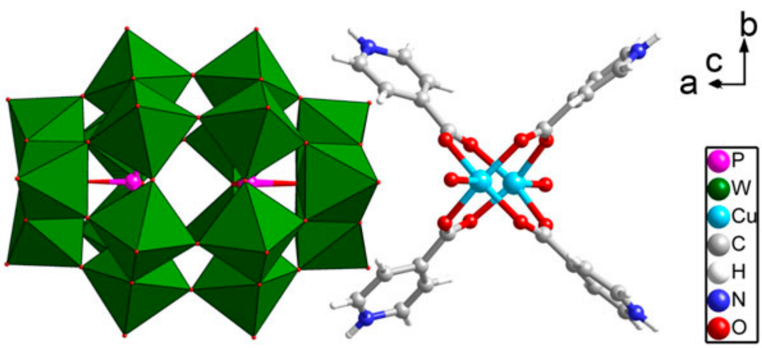

Figure 9. Polyhedron and ball-stick representations of the Wells–Dawson polyoxoanions and double paddle-wheel moiety in **4** (color code: P, purple; W, dark green; Cu, cyan; C, gray; H, white; N, blue O, red (see http://dx.doi.org/10.1080/00958972.2014.892592 for color version)).

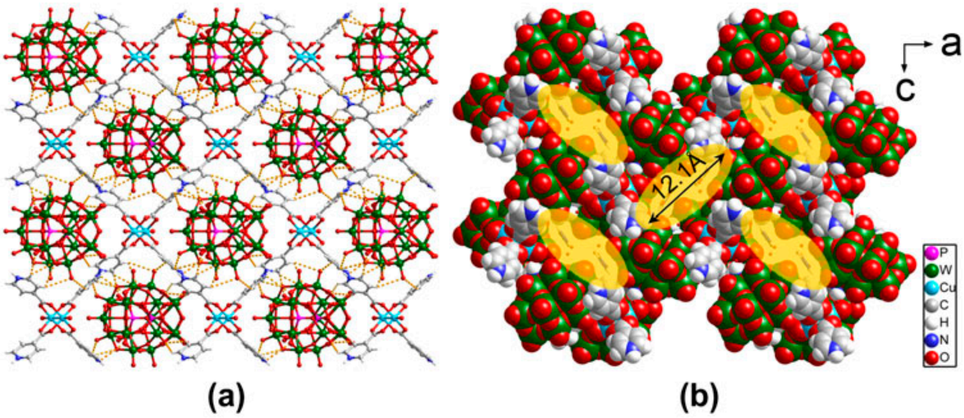

Figure 10. (a) Ball-stick representation of 3-D supramolecular network connected through hydrogen bonds and (b) space-filling representation with channels along the *b* axis of **4** (color code: P, purple; W, dark green; Cu, cyan; C, gray; H, white; N, blue O, red (see http://dx.doi.org/10.1080/00958972.2014.892592 for color version)).

Bond valence sum [22] calculation shows +2 Cu centers. Cu centers are bridged by four carboxylates from four ina molecules, forming a double paddle-wheel $\{Cu_2(Hina)_4(H_2O)_2\}$ (figure 9). As shown in figure 10, the connection of $\{Cu_2(Hina)_4(H_2O)_2\}$ units and $\{P_2W_{18}\}$ polyoxoanions forms microporous channels of 5.4×12.1 Å along the *b* axis. The discrete ina and water are located in the channels as guest molecules.

3.2. *Role of 4-bpo and Cu in the formation of 1–4*

According to the structure analyses above, 4-bpo ligands play important role in building the networks. The bidentate 4-bpo ligands connect coppers to form 1-D chain-like

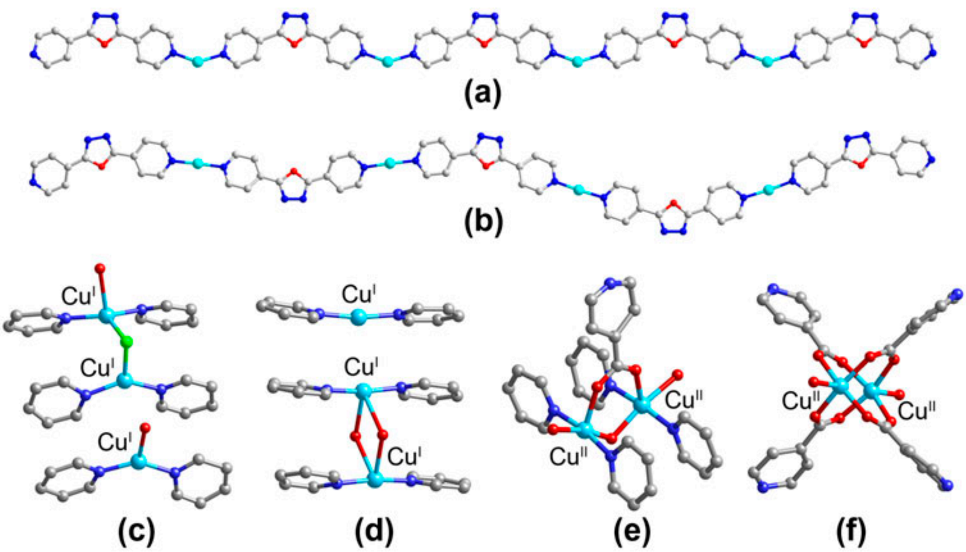

Figure 11. (a) The {Cu-(4-bpo)} unit in a side-by-side mode. (b) The {Cu-(4-bpo)} unit in an inversion mode. (c–f) The coordination geometries of Cu in **1–4**.

Downloaded by [Institute Of Atmospheric Physics] at 15:32 09 December 2014

{Cu-(4-bpo)} building units which display flexibility. Organic–inorganic hybrid moieties observed in 2-D layers of **1–3** are based on the {Cu-(4-bpo)} building unit. The {Cu(4-bpo) H_2O}$_n$ single chains in **1** are further modified by waters, and the double chains of {Cu_2(μ_2-Cl)(4-bpo)$_2$(H_2O)}$_n$ in **1** and {Cu_2(μ_2-OH)(4-bpo)$_2$(Hina)(H_2O)$_2$}$_n$ in **3** are linked by two {Cu-(4-bpo)} units through bridging groups, such as Cl, μ_2-OH, and ina. The rigid 2-D layers in **2** are constructed based on {Cu-(4-bpo)} through two bridging oxygens. There are two modes of connection between 4-bpo and Cu in {Cu-(4-bpo)} chains. The 4-bpo molecules in **1** are linked by Cu side-by-side to form a serrated chain [figure 11(a)], whereas the 4-bpo molecules in **2** and **3** are connected by Cu in an inversion fashion to form a wavy chain [figure 11(b)]. Combined with the structures that we have reported [18], these are contributed to the different template-effect of Keggin and Wells–Dawson polyoxoanions. The wavy chains in **2** and **3** better fit the shape of the large ellipsoidal Wells–Dawson polyoxoanions than the serrated chain. Additionally, these chains in the 2-D hybrid layers are arranged in a facial mode through π–π stacking. The multiple packing mode of heterocyclic 4-bpo is efficient in minimizing hindrance.

Cu^{II} is applied as a starting material in the synthesis of **1–4**. Bond valance sum calculations indicate that Cu^{II} ions are converted to Cu^{I} in **1** and **2** with a reduction under the hydrothermal condition in the presence of different reducers [25]. Cu ions display various coordination modes in **1–4**. The coordination numbers of Cu^{I} in **1** and **2** are two to four, which lead to linear, triangular, and seesaw coordination geometries as shown in [figure 11(c), (d)]. The Cu^{II} ions in **3** and **4** are five coordinate in square pyramidal geometry [figure 11(e), (f)]. The Cu coordination geometries are consistent with their oxidation state.

3.3. *Infrared spectroscopic study*

The IR spectrum of **1** (figure S5) exhibits the characteristic peaks of Keggin structure at 1018, 979, 925, and 784 cm^{-1} assigned to ν(Si–O), ν(W–O_d), ν(W–O_b–W), and ν(W–O_c–W), respectively [26]. In figures S6–S8, IR spectra of **2–4** have characteristic peaks of a Dawson structure. The peaks for ν(P–O), ν(W–O_d), ν(W–O_b–W), and ν(W–O_c–W) are at 1093, 962, 912, and 782 cm^{-1} in **2**, 1091, 960, 912, and 781 cm^{-1} in **3**, and 1089, 958, 910, and 779 cm^{-1} in **4**, respectively [27]. The IR results indicate that the structures of the POMs in **1–4** remain intact after the hydrothermal synthesis.

3.4. *XPS spectroscopic study*

XPS spectra of **1–4**, shown in figures S9–S12, have two peaks at 952.2 eV ($2p_{1/2}$) and 932.2 eV ($2p_{3/2}$) for **1** and **2**, which indicate Cu in +1 oxidation state (figures S9 and S10) [28]. Compound **3** shows two peaks at 953.6 eV ($2p_{1/2}$) and 933.8 eV ($2p_{3/2}$) and **4** shows two peaks at 953.8 eV ($2p_{1/2}$) and 934.0 eV ($2p_{3/2}$), which are attributed to Cu^{II} (figures S11 and S12). The appearance of the characteristic satellite peaks around 963 and 943 eV also represents Cu in **3** and **4** are +2 [29].

3.5. *Thermogravimetric analysis*

Thermogravimetric curves (figures S13–S16) show the thermal behaviors of **1–4**. The TG curve of **1** undergoes a slight weight loss before 320 °C and a continuous weight loss until 580 °C. The total weight loss of 22.62% of its initial weight corresponds to release of one lattice water, two coordination waters, two $(CH_3)_4N^+$, and three 4-bpo (Calcd 22.50%).

Downloaded by [Institute Of Atmospheric Physics] at 15:32 09 December 2014

Compound **2** has a total weight loss of 22.28% from 25 to 580 °C, which corresponds to release of six lattice waters, two $N(CH_3)_4^+$, and four 4-bpo (Calcd 22.17%). The TG curve of **3** undergoes a slight weight loss before 400 °C and continuous weight loss until 590 °C. The total weight loss of **3** is 24.50%, attributed to release of four lattice waters, four coordination waters, two ina, and four 4-bpo (Calcd 24.37%). Compound **4** has a total weight loss of 19.06% of its initial weight from 25 to 530 °C, corresponding to release of 11 lattice waters, two coordination waters, and five ina (Calcd 18.90%).

3.6. *Catalysis*

The catalytic activity of **1–4** for epoxidation of styrene was investigated with TBHP as oxidant (scheme 1). In order to compare catalytic activity, 0.005 mM of **1–4** was used for epoxidation. To distinguish the active species in **1–4**, the catalytic activity of $H_4SiW_{12}O_{40}$ and $H_6P_2W_{18}O_{62}$ with the same amount was also investigated.

Table 2 shows the conversion of styrene and the selectivities to styrene oxide, benzaldehyde, and other products. Catalysts **1–4** have very different catalytic performance compared to their corresponding polyoxoacids although the latter proceed as homogeneous systems. These results imply enhanced catalytic activities of POMs within organic–inorganic hybrid compounds. Also, **2–4** exhibit similar conversions of styrene, much higher than that of **1**, whereas **1** and **2** exhibit similar selectivities to styrene oxide which are much higher than those for **3** and **4**. Therefore, the catalytic performance of **1–4** is not directly related to the relative content(s) of Cu, POMs, and 4-bpo or ina of the catalysts. Catalysts **2–4** with high conversions of styrene possess Wells–Dawson type polyoxoanions and **1** with low conversion has a Keggin-type. Low conversions of styrene were also reported over other Keggin-based catalysts [15a, 18]. Catalysts **1** and **2** with high selectivities to styrene oxide contain Cu^I centers and catalysts **3** and **4** with low selectivities contain Cu^{II}. The effect of POMs is particularly obvious between **1** and **2** where both contain Cu^I in similar coordination geometries and similar 2-D hybrid layer but different polyoxoanions located between layers. Based on the above results, it may be implied that both Wells–Dawson type polyoxoanions and Cu^I centers play important roles in epoxidation of styrene. As catalyst **2** is the only

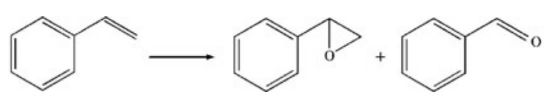

Scheme 1. Epoxidation of styrene to styrene oxide and benzaldehyde.

Table 2. Catalytic activities of **1–4** for epoxidation of styrene.

Catalyst	Conversion (%)	Selectivity to styrene oxide (%)	Selectivity to benzaldehyde (%)	Selectivity to benzoic acid and others (%)
1	48.2	60.2	34.7	5.1
2	73.2	69.4	26.4	4.2
3	76.7	33.0	61.4	5.6
4	70.3	22.9	71.0	6.1
$H_4SiW_{12}O_{40}$	31.7	47.9	50.7	1.4
$H_6P_2W_{18}O_{62}$	54.7	33.1	62.3	4.6

Downloaded by [Institute Of Atmospheric Physics] at 15:32 09 December 2014

compound containing both Wells–Dawson type polyoxoanions and Cu^{I} centers, it has the highest yield of styrene oxide.

Catalytic activity of the POMs-based hybrid compounds may be affected by many factors, including the individual components (POMs, metal ions, and ligands), the coordination mode and their oxidation state of the metal ions, the dimensionality and porosity of the structures, etc. Therefore, it is still a challenge to understand their catalytic behavior and requires further systematic investigation on the relationship between the catalytic performance and the structure and other properties of such hybrid compounds.

Studies on reusability of the catalysts show no significant loss in catalytic activity after three cycles. Compared with the simulated pattern from single-crystal data and the as-synthesized pattern, the typical powder XRD pattern of **2** after used is almost unchanged, which indicates the high stability of the catalyst during the reactions (figure S17).

4. Conclusion

We have isolated four POMs-based organic–inorganic compounds with zero, one, and 3-D structures under hydrothermal reactions. The coordination number of Cu varies from two to five in different environments. The 4-bpo ligands and Cu atoms are connected to form serrated chains in **1** and wavy chains in **2** and **3**, which meet the requirement of the POMs with different sizes. The catalytic activity of the four compounds for epoxidation of styrene demonstrates that Wells–Dawson POMs display higher conversion of styrene and the Cu^{I}-containing compounds exhibit better selectivity to styrene oxide.

Supplementary material

CCDC 868926–868929 contain the supplementary crystallographic data for **1–4**. These data can be obtained free of charge via http://www.ccdc.cam.ac.uk/conts/retrieving.html or from the Cambridge Crystallographic Data Center, 12 Union Road, Cambridge CB2 1EZ, UK; Fax: (+44) 1223-336-033; or E-mail: deposit@ccdc.cam.ac.uk. ORTEP diagrams, IR and XPS spectra, TG curves and crystalgraphical details of **1–4** are included in the supplementary data.

Funding

This work was supported by the National Natural Science Foundation [grant number 21371035], [grant number 21173050]; and the National Science Foundation for Young Scientists of China [grant number B010204].

References

[1] (a) I.V. Kozhevnikov. *Chem. Rev.*, **98**, 171 (1998); (b) T. Okuhara. *Chem. Rev.*, **102**, 3641 (2002); (c) Y.V. Geletii, B. Botar, P. Koegerler, D.A. Hillesheim, D.G. Musaev, C.L. Hill. *Angew. Chem. Int. Ed.*, **47**, 3896 (2008).
[2] (a) N. Mizuno, M. Misono. *Chem. Rev.*, **98**, 199 (1998); (b) A. Müller, S. Roy. *Coord. Chem. Rev.*, **245**, 153 (2003).

Downloaded by [Institute Of Atmospheric Physics] at 15:32 09 December 2014

[3] (a) A. Corma, H. García. *Chem. Rev.*, **102**, 3837 (2002); (b) Y. Ren, B. Yue, M. Gu, H. He. *Materials*, **3**, 764 (2010).
[4] (a) M. Nooraeipour, M. Moghadam, S. Tangestaninejad, V. Mirkhani, I. Mohammadpoor-Baltork, N. Iravani. *J. Coord. Chem.*, **65**, 226 (2012); (b) M. Zakeri, M. Moghadam, I. Mohammadpoor-Baltork, S. Tangestaninejad, V. Mirkhani, A.R. Khosropour. *J. Coord. Chem.*, **65**, 1144 (2012); (c) M. Bagherzadeh, M. Zare. *J. Coord. Chem.*, **65**, 4054 (2012); (d) A. Banaei, B. Rezazadeh. *J. Coord. Chem.*, **66**, 2129 (2013).
[5] P.X. Lei, C.C. Chen, J. Yang, W.H. Ma, J.C. Zhao, L. Zang. *Environ. Sci. Technol.*, **39**, 8466 (2005).
[6] Y. Izumi, K. Urabe. *Chem. Lett.*, **10**, 663 (1981).
[7] (a) N.M. Okun, T.M. Anderson, C.L. Hill. *J. Am. Chem. Soc.*, **125**, 3194 (2003); (b) N. Mizuno, K. Kamata, K. Yamaguchi. *Top. Catal.*, **53**, 876 (2010).
[8] B.R. Jermy, A. Pandurangan. *Appl. Catal. A*, **295**, 185 (2005).
[9] J. Juan-Alcañiz, E.V. Ramos-Fernandez, U. Lafont, J. Gascon, F. Kapteijn. *J. Catal.*, **269**, 229 (2010).
[10] Y. Izumi, R. Hasebe, K. Urabe. *J. Catal.*, **84**, 402 (1983).
[11] (a) X.L. Wang, C. Qin, E.B. Wang, Z.M. Su, Y.G. Li, L. Xu. *Angew. Chem. Int. Ed.*, **45**, 7411 (2006); (b) X.F. Kuang, X.Y. Wu, R.M. Yu, J.P. Donahue, J.S. Huang, C.Z. Lu. *Nature Chem.*, **2**, 461 (2010); (c) S.T. Zheng, J. Zhang, X.X. Li, W.H. Fang, G.Y. Yang. *J. Am. Chem. Soc.*, **132**, 15102 (2010); (d) B. Nohra, H. El Moll, L.M.R. Albelo, P. Mialane, J. Marrot, C. Mellot-Draznieks, M. O'Keeffe, R.N. Biboum, J. Lemaire, B. Keita, L. Nadjo, A. Dolbecq. *J. Am. Chem. Soc.*, **133**, 13363 (2011).
[12] (a) Y.P. Ren, X.J. Kong, X.Y. Hu, M. Sun, L.S. Long, R.B. Huang, L.S. Zheng. *Inorg. Chem.*, **45**, 4016 (2006); (b) S.L. Li, Y.Q. Lan, J.F. Ma, J. Yang, X.H. Wang, Z.M. Su. *Inorg. Chem.*, **46**, 8283 (2007); (c) J.Y. Niu, S.W. Zhang, H.N. Chen, J.W. Zhao, P.T. Ma, J.P. Wang. *Cryst. Growth Des.*, **11**, 3769 (2011).
[13] (a) S.T. Zheng, J. Zhang, G.Y. Yang. *Angew. Chem. Int. Ed.*, **47**, 3909 (2008); (b) L.M. Rodriguez-Albelo, A.R. Ruiz-Salvador, A. Sampieri, D.W. Lewis, A. Gómez, B. Nohra, P. Mialane, J. Marrot, F. Sécheresse, C. Mellot-Draznieks, R.N. Biboum, B. Keita, L. Nadjo, A. Dolbecq. *J. Am. Chem. Soc.*, **131**, 16078 (2009).
[14] C.Y. Sun, S.X. Liu, D.D. Liang, K.Z. Shao, Y.H. Ren, Z.M. Su. *J. Am. Chem. Soc.*, **131**, 1883 (2009).
[15] (a) F. Yu, X.J. Kong, Y.Y. Zheng, Y.P. Ren, L.S. Long, R.B. Huang, L.S. Zheng. *Dalton Trans.*, 9503 (2009); (b) F. Yu, P.Q. Zheng, Y.X. Long, Y.P. Ren, X.J. Kong, L.S. Long, Y.Z. Yuan, R.B. Huang, L.S. Zheng. *Eur. J. Inorg. Chem.*, 4526 (2010).
[16] D. Dutta, A.D. Jana, M. Debnath, A. Bhaumik, J. Marek, M. Ali. *Dalton Trans.*, 11551 (2010).
[17] J. Du, J.H. Yu, J.Y. Tang, J. Wang, W.X. Zhang, W.R. Thiel, M.J. Jia. *Eur. J. Inorg. Chem.*, 2361 (2011).
[18] Y.H. Ren, C.B. Du, S.J. Feng, C.L. Wang, Z.P. Kong, B. Yue, H.Y. He. *CrystEngComm*, **13**, 7143 (2011).
[19] (a) E.O. North. *Inorg. Synth.*, **1**, 129 (1939); (b) C.R. Graham, R.G. Finke. *Inorg. Chem.*, **47**, 3679 (2008).
[20] F. Bentiss, M. Lagrenée. *J. Heterocycl. Chem.*, **36**, 1029 (1999).
[21] G.M. Sheldrick, *SHELXL-97, A Program for Automatic Solution of Crystal Structure*, University of Gottingen, Germany (1997).
[22] I.D. Brown, D. Altermatt. *Acta Crystallogr. B*, **41**, 244 (1985).
[23] (a) J.Q. Sha, C. Wang, J. Peng, J. Chen, A.X. Tian, P.P. Zhang. *Inorg. Chem. Commun.*, **10**, 1321 (2007); (b) J.Q. Sha, J. Peng, Y.Q. Lan, Z.M. Su, H.J. Pang, A.X. Tian, P.P. Zhang, M. Zhu. *Inorg. Chem.*, **47**, 5145 (2008); (c) X.Y. Zhao, D.D. Liang, S.X. Liu, C.Y. Sun, R.G. Cao, C.Y. Gao, Y.H. Ren, Z.M. Su. *Inorg. Chem.*, **47**, 7133 (2008); (d) X.L. Wang, Y.G. Li, Y. Lu, H. Fu, Z.M. Su, E.B. Wang. *Cryst. Growth Des.*, **10**, 4227 (2010).
[24] X.L. Wang, H.L. Hu, A.X. Tian, H.Y. Lin, J. Li, L.M. Shi. *Inorg. Chem. Commun.*, **13**, 745 (2010).
[25] (a) C.M. Liu, D.Q. Zhang, D.B. Zhu. *Cryst. Growth Des.*, **5**, 1639 (2005); (b) K. Pavani, S.E. Lofland, K.V. Ramanujachary, A. Ramanan. *Eur. J. Inorg. Chem.*, **568**, (2007); (c) Y.Q. Lan, S.L. Li, X.L. Wang, K.Z. Shao, D.Y. Du, H.Y. Zang, Z.M. Su. *Inorg. Chem.*, **47**, 8179 (2008).
[26] (a) Y.B. Liu, Y. Wang, L.N. Xiao, Y.Y. Hu, L.M. Wang, X.B. Cui, J.Q. Xu. *J. Coord. Chem.*, **65**, 4342 (2012); (b) R. Yang, S.X. Liu, Q. Tang, S.J. Li, D.D. Liang. *J. Coord. Chem.*, **65**, 891 (2012); (c) X.L. Wang, C. Xu, H.Y. Lin, G.C. Liu, J. Luan, Z.H. Chang, A.X. Tian. *J. Coord. Chem.*, **66**, 1451 (2013).
[27] (a) C. Liang, Y. Lu, H. Fu, W.L. Chen, E.B. Wang. *J. Coord. Chem.*, **65**, 3254 (2012); (b) Y.L. Xu, K. Yu, B.B. Zhou, Z.H. Su, J. Wu. *J. Coord. Chem.*, **66**, 1303 (2013).
[28] J. Batista, A. Pintar, D. Mandrino, M. Jenko, V. Martin. *Appl. Catal. A-Gen.*, **206**, 113 (2001).
[29] J.X. Zhou, L.Y. Guo, X.W. Guo, J.B. Mao, S.G. Zhang. *Green Chem.*, **12**, 1835 (2010).

Downloaded by [Institute Of Atmospheric Physics] at 15:32 09 December 2014